

AD/A-004 047

ANALYSIS AND SYNTHESIS OF SPATIAL FILTERS  
THAT HAVE CHEBYSHEV CHARACTERISTICS

Robert J. Mailloux

Air Force Cambridge Research Laboratories  
Hanscom Air Force Base, Massachusetts

13 September 1974

DISTRIBUTED BY:



National Technical Information Service  
U. S. DEPARTMENT OF COMMERCE

Unclassified

SECURITY CLASSIFICATION OF THIS PAGE (When Data Entered)

REPORT DOCUMENTATION PAGE		READ INSTRUCTIONS BEFORE COMPLETING FORM	
1. REPORT NUMBER <b>AFCRL-TR-74-0455</b>	2. GOVT ACCESSION NO.	3. RECIPIENT'S CATALOG NUMBER <b>ADA-004041</b>	
4. TITLE (and Subtitle) <b>ANALYSIS AND SYNTHESIS OF SPATIAL FILTERS THAT HAVE CHEBYSHEV CHARACTERISTICS</b>		5. TYPE OF REPORT & PERIOD COVERED <b>Scientific. Interim.</b>	
6. PERFORMING ORG REPORT NUMBER <b>PSRP No. 601</b>		7. AUTHOR(s) <b>Robert J. Mailloux</b>	
8. CONTRACT OR GRANT NUMBER(s)		9. PERFORMING ORGANIZATION NAME AND ADDRESS <b>Air Force Cambridge Research Laboratories (LZR) Hanscom AFB Massachusetts 01731</b>	
10. PROGRAM ELEMENT, PROJECT, TASK AREA & WORK UNIT NUMBERS <b>62702F, 674600 46001301</b>		11. CONTROLLING OFFICE NAME AND ADDRESS <b>Air Force Cambridge Research Laboratories (LZR) Hanscom AFB Massachusetts 01731</b>	
12. REPORT DATE <b>13 September 1974</b>		13. NUMBER OF PAGES <b>34</b>	
14. MONITORING AGENCY NAME & ADDRESS(if different from Controlling Office)		15. SECURITY CLASS (of this report) <b>Unclassified</b>	
		16. DECLASSIFICATION/DOWNGRADING SCHEDULE	
16. DISTRIBUTION STATEMENT (of this Report)  <b>Approved for public release; distribution unlimited.</b>			
17. DISTRIBUTION STATEMENT (of the abstract entered in Block 20, if different from Report)			
18. SUPPLEMENTARY NOTES			
19. KEY WORDS (Continue on reverse side if necessary and identify by block number) <b>Spatial filters Stratified dielectrics Chebyshev filters Multiple-beam antenna arrays Limited sector-scanning</b> <b>Airport PAR systems Synchronous satellite communication antennas</b>			
20. ABSTRACT (Continue on reverse side if necessary and identify by block number) <b>Stratified dielectric filters in the spatial domain are being synthesized by a new Chebyshev technique recently developed at AFCRL. Used as radomes at the face of an array, these filters can control the residual grating lobes that plague limited sector-scanning and multiple-beam arrays in airport precision-approach radar (PAR) systems and synchronous satellite communications antennas. Formulas and charts are given for designing two-, three-, and four-layer filters. The characteristics of several four-layer filters are compared and discussed.</b>			

DD FORM 1 JAN 73 1473 EDITION OF 1 NOV 68 IS OBSOLETE

Unclassified

Unclassified SECURITY CLASSIFICATION OF THIS PAGE (DoD Form 1) 1000

**PRICES SUBJECT TO CHANGE**

Reproduced by  
**NATIONAL TECHNICAL  
INFORMATION SERVICE**  
US Department of Commerce  
Springfield, VA 22151

## **Preface**

The use of stratified dielectrics as spatial filters was originally suggested by Dr. A. C. Schell.

**Preceding page blank**

## Contents

1. INTRODUCTION	7
2. PROPAGATION CHARACTERISTICS OF STRATIFIED DIELECTRICS WITH PLANE-WAVE INCIDENCE AT ARBITRARY ANGLE	8
2.1 General Formulation; Choice of Coordinate Systems	8
2.2 Wave Matrices and Transmission Through Stratified Dielectric Filters	14
3. CHEBYSHEV FILTER SYNTHESIS	18
3.1 General Procedures	18
3.2 The Mathematics of Filter Synthesis	18
3.2.1 Two-Layer Filters	19
3.2.2 Three-Layer Filters	20
3.2.3 Four-Layer Filters	21
3.3 Filter Design	22
3.4 Results Obtained With Two Filters	26
3.5 Results Obtained With an Array of Parallel-Plane Waveguides	29
4. CONCLUSIONS	31
REFERENCES	31
APPENDIX A: Radiated Field of infinite Array	33
APPENDIX B: Wave Matrix Definitions for Parallel and Perpendicular Polarization	35

Preceding page blank

## Illustrations

1. Array Geometry Showing Array Coordinates $\theta, \phi$ and Polarization Coordinates $\Theta, \Phi$	9
2. Interface Between Two Dielectric Media	14
3. Basic Filter Section	16
4. Two-Layer Chebyshev Filter Rejection	23
5. Three-Layer Chebyshev Filter Rejection	23
6. Four-Layer Chebyshev Filter Rejection	24
7. Reflection Coefficients for Two-Layer Chebyshev Filter	24
8. Reflection Coefficients for Three-Layer Chetyshev Filter	25
9. Reflection Coefficients for Four-Layer Chebyshev Filter	25
10. Transmission Characteristics of Four-Layer Chebyshev Filter ( $S = 0.5\lambda$ )	27
11. Transmission Characteristics of Four-Layer Chebyshev Filter ( $S = \lambda$ )	28
12. Limited-Scan Array Grating Lobe Amplitude Locus	30

## **Analysis and Synthesis of Spatial Filters That Have Chebyshev Characteristics**

### **1. INTRODUCTION**

Spatial filters, designed by a new Chebyshev synthesis technique recently developed at AFCRL, are being made of stratified dielectrics. These filters have successfully suppressed wide-angle sidelobe structures, particularly in phased-array antennas scanning a low sidelobe beam over a limited spatial sector. The wide-angle sidelobes, which are in fact grating lobes that have been suppressed to the -12 to -16 dB levels, are reduced to levels of approximately -20 dB without degradation of the near-broadside radiation characteristics of the array. Since the array face is flat, the optimal spatial filter consists of uniform layers of dielectric material properly spaced, having dielectric constants suitable to the required spatial discrimination.

Such filters also have application in radomes, which usually require wide-angle scan. Although the subject has not been addressed directly in this work, the equations and figures given here can also be applied to the design of filters intended for radome purposes.

---

(Received for publication 13 September 1974)

The principles of layered-dielectric frequency-domain filters and impedance transformers are now well established,<sup>1-5</sup> and insofar as possible the techniques for analysis and synthesis in this domain have been extended to the spatial domain. The fundamental difference between synthesis in the frequency domain and synthesis in the spatial domain arises because the transmission coefficients of layers that have a high dielectric constant are strongly frequency-dependent but relatively invariant with the spatial angle of incidence: if a wave from a medium of low dielectric constant is incident on a medium of high dielectric constant, then for any angle of incidence the wave propagation angle in the latter is almost perpendicular to the interface.

This distinction suggested a fundamental change in filter design. The frequency-domain transformers and filters synthesized by Collin and others<sup>1-5</sup> consisted of various dielectric layers sandwiched together. The spatial domain filters synthesized in the work reported here consist of quarter-wave sections of dielectric separated by half-wave or full-wave air spaces. The methods that Collins outlined in two basic studies<sup>1,6</sup> were applied in their development.

## 2. PROPAGATION CHARACTERISTICS OF STRATIFIED DIELECTRICS WITH PLANE-WAVE INCIDENCE AT ARBITRARY ANGLE

### 2.1 General Formulation; Choice of Coordinate Systems

The end result of this analysis is a technique for synthesizing spatial filters that control the radiation pattern of a phased array used for limited-sector scan. For convenience, all propagation coordinates are referred to the basic reference coordinates  $x, y, z$  of the array (Figure 1), which excites a spectrum of plane waves and evanescent plane waves as described in Appendix A. For purposes of this analysis, we need consider only a single wave radiating in the direction of the vector

$$\bar{k} = \hat{x}k_x + \hat{y}k_y + \hat{z}k_z = \hat{k}k_o, \quad (1)$$

1. Collin, R. E. (1955) Theory and design of wideband multisection quarter-wave transformers, Proc. IRE 43(No. 2):179-185, Feb. 1955.
2. Cohn, S. B. (1955) Optimum design of stepped transmission-line transformers, IRE Tr. MTT MTT-3(No. 2):16-21, Apr. 1955.
3. Riblett, H. J. (1957) General synthesis of quarter-wave impedance transformers, IRE Tr. MTT MTT-5(No. 1):36-43, Jan. 1957.
4. Young, L. (1959) Tables for cascaded homogeneous quarter-wave transformers, IRE Tr. MTT MTT-7(No. 2):233-244, Apr. 1959.
5. Young, L. (1962) Stepped-impedance transformers and filter prototypes, IRE Tr. MTT MTT-10(No. 5):339-359, Sept. 1962.
6. Collin, R. E. (1960) Field Theory of Guided Waves, McGraw-Hill, pp. 79-93.

where

$$k_x = k_0 u_o = k_0 (\sin \theta_o \cos \phi_o),$$

$$k_y = k_0 v_o = k_0 (\sin \theta_o \sin \phi_o),$$

$$k_z = k_0 \cos \theta_o,$$

$$k_0 = 2\pi/\lambda,$$

with  $u_o$  and  $v_o$  the direction cosines.

The aperture field of the phased array is assumed to be polarized in the  $y$  direction, thus determining the polarization of the incident plane waves. This radiation is best described by the  $\Theta, \Phi, r$  coordinates of Figure 1 because in the absence of the dielectric layers the farfield radiation of the array contains only an  $E_\Phi$  term. The  $\Phi$  angle is measured in the  $yz$  plane; the  $\Theta$  angle, from the positive  $x$  axis. In general, the vector  $\bar{A}'$  in  $\Theta, \Phi, r$  space is obtained from the vector  $\bar{A}$  in  $x, y, z$  space by the dyadic relation:

$$\begin{aligned} \bar{A}' &= \hat{\Theta} A'_\Theta + \hat{\Phi} A'_\Phi + \hat{r} A'_r \\ &= \underline{T} \cdot \bar{A}, \end{aligned} \quad (2)$$

where  $\underline{T}$  is the nine-component dyad written:

$$\begin{aligned} \underline{T} &= \hat{\Theta} (-\hat{x} \sin \Theta + \hat{y} \cos \Phi \cos \Theta + \hat{z} \sin \Phi \cos \Theta) + \\ &\quad + \hat{\Phi} (0 - \hat{y} \sin \Phi + \hat{z} \cos \Phi) + \\ &\quad + \hat{r} (\hat{x} \cos \Theta + \hat{y} \cos \Phi \sin \Theta + \hat{z} \sin \Phi \sin \Theta). \end{aligned} \quad (3)$$

This expression, a formalized way of describing the relationship between the various components of the vectors along the unit vector directions, is equivalent to the matrix representation:

$$\begin{pmatrix} A'_\Theta \\ A'_\Phi \\ A'_r \end{pmatrix} = \begin{pmatrix} -\sin \Theta & \cos \Phi \cos \Theta & \sin \Phi \cos \Theta \\ 0 & -\sin \Phi & \cos \Phi \\ \cos \Theta & \cos \Phi \sin \Theta & \sin \Phi \sin \Theta \end{pmatrix} \begin{pmatrix} A_x \\ A_y \\ A_z \end{pmatrix}. \quad (4)$$

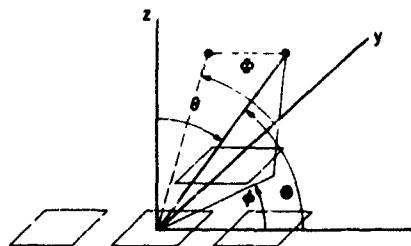


Figure 1. Array Geometry Showing Array Coordinates  $\theta, \phi$  and Polarization Coordinates  $\Theta, \Phi$

This statement of equivalence to a matrix transformation indicates that the process of taking the inverse of a dyad is the same as that for a matrix; and that the transformation of a vector from one system to a second, and from that system to a third, is obtained through matrix multiplication of the rows and columns of the matrix forms or, equivalently, through scalar multiplication of the dyad by the second transforming dyad. As with the equivalent matrix operation, dyad multiplication is not commutative. Relating the two systems in general by

$$\begin{aligned}\sin \Theta &= \sqrt{1 - \sin^2 \theta \cos^2 \phi}, \\ \cos \Theta &= \sin \theta \cos \phi, \\ \sin \Phi &= \frac{\cos \theta}{\sqrt{1 - \sin^2 \theta \cos^2 \phi}}, \\ \cos \Phi &= \frac{\sin \theta \sin \phi}{\sqrt{1 - \sin^2 \theta \cos^2 \phi}}.\end{aligned}\tag{5}$$

and specifically restricting the  $\theta, \phi$  parameters to  $\theta_0, \phi_0$  (the direction of the main beam of the array), yields the dyad in the righthand rectangular coordinate system  $\Theta_0, \Phi_0, r_0$ , as follows:

$$\begin{aligned}T_0 &= \hat{\Theta}_0 \left( -\hat{x} \frac{\sqrt{1-u_0^2}}{u_0} + \hat{y} \frac{u_0 v_0}{\sqrt{1-u_0^2}} + \hat{z} \frac{u_0 \cos \Theta_0}{\sqrt{1-u_0^2}} \right) + \\ &+ \hat{\Phi}_0 \left( 0 - \hat{y} \frac{\cos \Theta_0}{\sqrt{1-u_0^2}} + \hat{z} \frac{v_0}{\sqrt{1-u_0^2}} \right) + \\ &+ \hat{r}_0 (\hat{x} u_0 + \hat{y} v_0 + \hat{z} \cos \Theta_0).\end{aligned}\tag{6}$$

This choice of coordinates makes the unit vector  $\hat{r}_0$  coincide with the direction of propagation. Thus,  $\hat{r}_0 = \hat{k}$ . Transformed by this dyadic operation into the new coordinate system, the plane wave (see Appendix A) is linearly polarized, and has the following electric and magnetic fields:

$$\begin{aligned}\mathbf{E}' &= \hat{\Phi}_0 \mathbf{E}_{\Phi_0} = \hat{\Phi}_0 \mathbf{C}(\theta_0, \phi_0) e^{-jkr_0}, \\ \mathbf{B}' &= \hat{\Theta}_0 \mathbf{B}_{\Theta_0} = \hat{\Theta}_0 \left( \frac{k_0^2}{2\pi\omega} \right) \mathbf{C}(\theta_0, \phi_0) e^{-jkr_0},\end{aligned}\tag{7}$$

where  $r_0$  is a distance measured in the direction of propagation, and  $C(\theta_0, \phi_0)$  is a parameter (evaluated in Appendix A) for multiplying each wave.

Throughout this report the  $\Theta_0, \Phi_0, r_0$  system is used for describing polarization of the wave. For describing propagation in the dielectric layers, it is more convenient to resolve the fields into components along the spherical coordinate system  $\hat{\Theta}, \hat{\Phi}, \hat{r}$ . As before, the subscripted dyad  $\underline{R}_0$  is used when  $\hat{r}$  coincides with  $\hat{r}_0$ . These are the conventional definitions of perpendicular and parallel polarizations for arbitrary incidence of a plane wave on a dielectric slab.

In general  $\theta, \phi, r$  coordinates the vector  $\bar{A}''$  is related to  $\bar{A}$  in the original  $x, y, z$  coordinates by the dyadic relation:

$$\bar{A}'' = \underline{T}' \cdot \bar{A}, \quad (8)$$

where

$$\begin{aligned} \underline{T}' = & \hat{\theta} (\hat{x} \cos \phi \cos \theta + \hat{y} \sin \phi \cos \theta - \hat{z} \sin \theta) + \\ & + \hat{\phi} (-\hat{x} \sin \phi + \hat{y} \cos \phi + 0) + \\ & + \hat{r} (\hat{x} u + \hat{y} v + \hat{z} \cos \theta). \end{aligned}$$

It is sometimes convenient to transform vectors from one system to the other. Unit vectors in the  $\hat{\theta}, \hat{\phi}, \hat{r}$  coordinate system are related to those in the  $\hat{\Theta}, \hat{\Phi}, \hat{r}$  system by a rotation  $-\delta$  about the  $\hat{r}$ , and so the vector  $\bar{A}''$  in the first system is written in terms of the vector  $\bar{A}'$  in the second system by means of the dyadic notation:

$$\bar{A}'' = \underline{R} \cdot \bar{A}', \quad (9)$$

where

$$\begin{aligned} \underline{R} = & \hat{\theta} (\hat{\Theta} \cos \delta - \hat{\Phi} \sin \delta) + \\ & + \hat{\phi} (\hat{\Theta} \sin \delta + \hat{\Phi} \cos \delta) + \\ & + \hat{r} \hat{r}. \end{aligned}$$

The required angle  $\delta$  is obtained by aligning the unit vector  $\hat{\phi}$  parallel to the plane of the dielectric layer. Then, when transformed by the dyad  $\underline{R} \cdot \underline{T}$  into the  $\theta, \phi, r$  system, the unit vector  $\hat{z}$  is perpendicular to  $\hat{\phi}$ , and

$$\hat{\phi} \cdot \underline{R} \cdot \underline{T} \cdot \hat{z} = 0. \quad (10)$$

Solution of this equation yields values of  $\delta$  defined by the following equations:

$$\sin \delta = \frac{\sin \phi}{\sqrt{1-u^2}}; \quad \cos \delta = \frac{-\cos \phi \cos \theta}{\sqrt{1-u^2}}. \quad (11)$$

Equation (8) could also have been obtained by letting the rotation dyad  $\underline{R}$  operate on a vector in the  $\Theta, \Phi, r$  system, with the result:

$$\bar{A}'' = \underline{T}' \cdot \bar{A} = \underline{R} \cdot \underline{I} \cdot \bar{A}. \quad (12)$$

Applying the transformation in Eq. (8) to the phased-array fields (see Appendix A) leads to the following resolution into two sets of plane-wave fields as evaluated along the  $\bar{k}$  path.

Parallel Polarization	Perpendicular Polarization
$E_{\theta_o} = \frac{-C(\theta_o, \phi_o) \sin \phi_o}{\sqrt{1-u_o^2}} e^{-jk_o r_o};$	$E_{\phi_o} = \frac{-C(\theta_o, \phi_o) \cos \phi_o \cos \theta_o}{\sqrt{1-u_o^2}} e^{-jk_o r_o};$
$B_{\phi_o} = E_{\theta_o} (k_o/\omega);$	$B_{\phi_o} = E_{\theta_o} (-k_o/\omega);$
$B_{r_o} = E_{r_o} = 0.$	

(13)

As noted by Collin,<sup>6</sup> parallel- and perpendicular-polarized waves propagate independently through the air-dielectric slab interface, and can be recombined at the output of the layered region to form a set of plane waves in  $\Theta_o, \Phi_o$  space, but the set will in general no longer be linearly polarized. The amplitude of the cross-polarized signal induced by the dielectric slabs is crucial to the spatial filter geometry, and is easily related to the scattering parameters of the filter. Based on the plane-wave filter transmission and reflection coefficients, the plane wave amplitudes at the output of the filter are given by:

Parallel Polarization	Perpendicular Polarization
$E_{\theta}^{OUT} = E_{\theta_o} T_{par};$	$E_{\phi}^{OUT} = E_{\phi_o} T_{prp};$
$B_{\phi}^{OUT} = B_{\phi_o} T_{par};$	$B_{\theta}^{OUT} = B_{\theta_o} T_{prp}.$

(14)

where  $T_{\text{par}}$  or  $T_{\text{prp}}$  are the filter transmission coefficients. The electric fields reflected toward the array by the filter interface are  $\Gamma_{\text{prp}}$  times the incident perpendicular polarization and  $\Gamma_{\text{par}}$  times the incident parallel polarized signal, given by:

Parallel Polarization	Perpendicular Polarization
$E_{\theta}^{\text{REF}} = E_{\theta_0} \Gamma_{\text{par}}$ ;	$E_{\phi}^{\text{REF}} = E_{\phi_0} \Gamma_{\text{prp}}$ ;
$B_{\phi}^{\text{REF}} = B_{\phi_0} \Gamma_{\text{par}}$ ;	$B_{\theta}^{\text{REF}} = -B_{\theta_0} \Gamma_{\text{prp}}$ .

(15)

The filter parameters  $\Gamma_{\text{par}}$ ,  $T_{\text{par}}$  and  $\Gamma_{\text{prp}}$ ,  $T_{\text{prp}}$  are evaluated in Sec. 2.2.

The inverse of the rotation dyadic  $R$  is used to transform the scattered field components back to the  $\Theta, \Phi, r$  coordinate system by changing any vector  $\bar{A}''$  in the  $\theta_0, \phi_0, r_0$  coordinates to the vector  $\bar{A}'$  such that

$$\bar{A}' = R^{-1} \cdot \bar{A}'', \quad (16)$$

where

$$\begin{aligned} R^{-1} = & \hat{\Theta}(\hat{\theta} \cos \delta + \hat{\phi} \sin \delta) + \\ & \times \hat{\Phi}(-\hat{\theta} \sin \delta + \hat{\phi} \cos \delta) + \\ & + \hat{r} \hat{r}. \end{aligned}$$

Hence,

$$\begin{aligned} \bar{A} = & \left[ \hat{\Theta} \left( -\hat{\theta} \frac{\cos \phi \cos \theta}{\sqrt{1-u^2}} + \hat{\phi} \frac{\sin \phi}{\sqrt{1-u^2}} \right) + \right. \\ & \left. + \hat{\Phi} \left( -\hat{\theta} \frac{\sin \phi}{\sqrt{1-u^2}} - \hat{\phi} \frac{\cos \phi \cos \theta}{\sqrt{1-u^2}} \right) + \hat{r} \hat{r} \right] \cdot \bar{A}'' . \end{aligned} \quad (17)$$

Using this dyadic transformation, with  $\hat{r}$  taken along the direction of propagation, and using the definition of the parallel- and perpendicular-polarized incident fields  $E_{\theta_0}$  and  $E_{\phi_0}$ , yields the following expressions for the transmitted  $E_{\phi_0}$  and cross-polarized  $E_{\theta_0}$  fields at the filter output:

$$\begin{aligned}
 \bar{E} &= C(\theta_0, \phi_0) e^{-jkr_0} \left[ \hat{\Theta}_0 \left( \frac{\sin \phi_0 \cos \phi_0 \cos \theta_0}{1 - u_0^2} \right) (T_{\text{par}} - T_{\text{prp}}) + \right. \\
 &\quad \left. + \hat{\Phi}_0 \left( \frac{\sin^2 \phi_0}{1 - u_0^2} T_{\text{par}} + \frac{\cos^2 \phi_0 \cos^2 \theta_0}{1 - u_0^2} T_{\text{prp}} \right) \right] \\
 &= C(\theta_0, \phi_0) e^{-jkr_0} \left[ \hat{\Theta}_0 K + \hat{\Phi}_0 K_{\text{cross}} \right], \tag{18}
 \end{aligned}$$

where  $K$  and  $K_{\text{cross}}$  are the filter transmission coefficients from the incident  $E_{\Theta_0}$ -linearly polarized field into  $\Theta_0$ - and cross-polarized ( $\Phi_0$ -polarized) fields. The reflected fields for these two polarizations are given by the same expressions as in Eq.(18), but with the transmission factors  $T_{\text{par}}$  and  $T_{\text{prp}}$  replaced by the filter reflection coefficients  $\Gamma_{\text{par}}$  and  $\Gamma_{\text{prp}}$ . These new filter coupling coefficients are defined as  $\mathcal{F}$  and  $\mathcal{F}_{\text{cross}}$ . By means of these expressions it can be shown that since energy is conserved for the two polarizations separately ( $T_{\text{par}}^* T_{\text{par}} + \Gamma_{\text{par}}^* \Gamma_{\text{par}} = 1$ ; and  $T_{\text{prp}}^* T_{\text{prp}} + \Gamma_{\text{prp}}^* \Gamma_{\text{prp}} = 1$ ), it is conserved within the system totally. Consequently,

$$KK^* + K_{\text{cross}} K_{\text{cross}}^* + \mathcal{F}\mathcal{F}^* + \mathcal{F}_{\text{cross}} \mathcal{F}_{\text{cross}}^* = 1. \tag{19}$$

## 2.2 Wave Matrices and Transmission Through Stratified Dielectric Filters

Quarter-wave transformers with Chebyshev behavior throughout a given frequency passband were synthesized by Collin<sup>1</sup> in 1955. The process has since been refined,<sup>2-5</sup> and there now exists an extensive tabulation of transformer parameters for various design specifications. Spatial filter design is similar in concept to bandpass filter design, except for some differences that will be taken up when filter design procedures are introduced.

Collin used the wave matrix formalism to derive convenient expressions for the transmission properties of layered impedance sections,<sup>1</sup> and to describe the spatial properties of abutting dielectric layers.<sup>6</sup>

The same formalism will be used here to derive properties of the stratified dielectric filters.

Figure 2 represents two dielectric media, showing incident and reflected waves  $a_1$  and  $b_1$  in medium 1, and incident and reflected waves  $a_2$  and  $b_2$  in medium 2. The incident waves are assumed to be either parallel-polarized or perpendicular-polarized, with no cross-polarized

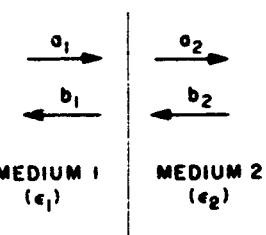


Figure 2. Interface Between Two Dielectric Media

components excited. In this case a purely algebraic relation exists between input and output. By the wave matrix, parameters  $a_1$  and  $b_1$  of medium 1 are related to parameters  $a_2$  and  $b_2$  of medium 2 in such a way that cascaded networks or layers are conveniently analyzed. The input-output parameters are thus related by:

$$\begin{pmatrix} a_1 \\ b_1 \end{pmatrix} = \begin{pmatrix} A_{11} & A_{12} \\ A_{21} & A_{22} \end{pmatrix} \begin{pmatrix} a_2 \\ b_2 \end{pmatrix}. \quad (20)$$

Collin<sup>1</sup> gives the obvious relations between the parameters  $A_{mn}$  of this matrix in terms of those of the conventional scattering matrix (see Appendix B), and shows that the wave matrix for a cascade of networks is the product of the wave matrices of each network. The parameter

$$A_{11} = \left. \frac{a_1}{a_2} \right|_{b_2=0}, \quad (21)$$

the inverse of the filter transmission coefficient, is of particular importance in filter design. The square of the absolute value of this parameter, the power loss ratio, will be considered extensively in the next section.

The normalizations of signal parameters required to convert the electromagnetic boundary value equations for parallel- and perpendicular-polarized waves into the proper format for wave matrix application are given in Appendix B. These result in the following equation for a junction between two dielectric materials:

$$\begin{pmatrix} a_1 \\ b_1 \end{pmatrix} = \frac{1}{T_1} \begin{pmatrix} 1 & \Gamma_1 \\ \Gamma_1 & 1 \end{pmatrix} \begin{pmatrix} a_2 \\ b_2 \end{pmatrix}, \quad (22)$$

where

$$\Gamma_1 = \frac{(1 - z_1/z_2)}{(1 + z_1/z_2)}$$

and

$$T_1 = 1 + \Gamma_1;$$

and where

$$z_j = \frac{k_{zj}}{k_{\epsilon_j}^2 \cos \theta}$$

for parallel polarization, and

$$z_j = \frac{\cos \theta}{k_{zj}}$$

for perpendicular polarization, and where

$$k_{zj} = k_0 \sqrt{\epsilon_j - \sin^2 \theta}$$

and

$$k_{\epsilon_j} = k_0 \sqrt{\epsilon_j}.$$

Here,  $\Gamma_1$  is the reflection coefficient at terminal 1, and  $T_1$  is the transmission coefficient from terminal 1 into terminal 2. The parameter  $\theta$  is defined for the incident medium air. Note that if the materials in sections 1 and 2 were reversed in position,  $\Gamma_1$  in the matrix would be replaced by  $-\Gamma_1$ , and  $T_1$  would be replaced by  $T_2 = 1 - \Gamma_1$ .

The wave matrix for a line of electrical length  $k_{zj} L$  is:

$$\begin{pmatrix} jk_{zj} L & 0 \\ e^{-jk_{zj} L} & e^{jk_{zj} L} \end{pmatrix} \quad (23)$$

Thus, for a filter section (Figure 3) consisting of a terminating air-dielectric interface between a dielectric layer of thickness  $t$ , and an air space of thickness  $s$ , the wave matrix relating the parameters  $a_1, b_1$  below the air space to the signals at the output terminal  $(a_2, b_2)$  can be written:

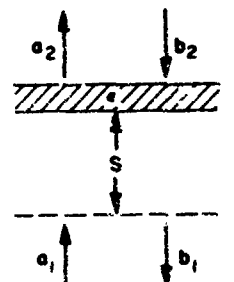


Figure 3. Basic Filter Section

$$\begin{pmatrix} jk_{z0} S & 0 \\ e^{-jk_{z0} S} & e^{jk_{z0} S} \end{pmatrix} \left[ \frac{1}{T_1} \begin{pmatrix} 1 & \Gamma_1 \\ \Gamma_1 & 1 \end{pmatrix} \begin{pmatrix} jk_{z\epsilon} t & 0 \\ e^{-jk_{z\epsilon} t} & e^{jk_{z\epsilon} t} \end{pmatrix} \right] \left[ \frac{1}{T_2} \begin{pmatrix} 1 & -\Gamma_1 \\ -\Gamma_1 & 1 \end{pmatrix} \right], \quad (24)$$

which leads to

$$\begin{aligned} [A(S, \epsilon, t)] &= \begin{pmatrix} A_{11} & A_{12} \\ A_{21} & A_{22} \end{pmatrix} \\ &= \frac{1}{T_1 T_2} \begin{pmatrix} e^{jkz_0 S} \left( e^{jkz_\epsilon t} - \Gamma_1^2 e^{-jkz_\epsilon t} \right) & -e^{jkz_0 S} \Gamma_1 \left( e^{jkz_\epsilon t} - e^{-jkz_\epsilon t} \right) \\ \Gamma_1 e^{-jkz_0 S} \left( e^{jkz_\epsilon t} - e^{-jkz_\epsilon t} \right) & e^{-jkz_0 S} \left( -\Gamma_1^2 e^{jkz_\epsilon t} + e^{-jkz_\epsilon t} \right) \end{pmatrix}. \quad (25) \end{aligned}$$

This dielectric layer and an air space constitute the basic element of the spatial filters considered in this report. The structure is more general than those considered in the previous literature because the goal here is to study spatial filtering, not frequency bandpass-filtering. It will be shown that without air spaces it is difficult to get any pronounced spatial behavior over narrow angular sectors.

Equation (25) can be rewritten in terms of the scattering parameters  $S_{11}$  and  $S_{12}$  for the special case of broadside incidence on a quarter-wave slab thickness, as follows:

$$A = \frac{1}{S_{12}} \begin{pmatrix} jkz_0 S & jkz_0 S \\ e^{jkz_0 S} & -S_{11} e^{jkz_0 S} \\ -jkz_0 S & -jkz_0 S \\ S_{11} e^{-jkz_0 S} & -e^{-jkz_0 S} \end{pmatrix}, \quad \text{where} \quad \begin{aligned} S_{11} &= \frac{\epsilon - 1}{\epsilon + 1} \\ S_{12} &= \frac{-2j\sqrt{\epsilon}}{\epsilon + 1} \end{aligned} \quad (26)$$

The wave matrix of a filter comprised of a number of such sections is obtained simply by multiplying the filter-section waves in the sequential order of the positions of their matrices  $A(S, \epsilon, t)$  in the filter (omitting the input section of line where appropriate). For example,

$$[A]_{\text{FILTER}} = \prod_{n=1}^N A(S_n, \epsilon_n, t_n). \quad (27)$$

Such generalized filter wave matrices are used here in two ways: (1) in the Chebyshev synthesis procedure, they are used for computing the filter power loss ratio; (2) with Eq.(B3) they are used for deriving the filter scattering parameters ( $\Gamma_{\text{par}}$ ,  $T_{\text{par}}$ ;  $\Gamma_{\text{prp}}$ , and  $T_{\text{prp}}$ ) for the parallel and perpendicular polarizations. These parameters are then used in Eq.(18) to define the desired and cross-polarized signals at the output of the filter.

### 3. CHEBYSHEV FILTER SYNTHESIS

#### 3.1 General Procedures

Collin's<sup>1</sup> procedure for transformer synthesis depends on the demonstrated properties of the polynomial expression for the power loss ratio, defined by Collin as the power ratio associated with the inverse of the filter transmission coefficient:

$$P = A_{11} A_{11}^* \quad (28)$$

Using filter elements consisting of sections of transmission line, each quarter-wavelength long at the design frequency, Collin proved that the power loss ratio was an even polynomial of  $\cos k_z t$  of degree  $2n$ , where  $n$  is the number of sections in the filter. He also showed that the power loss polynomial could be written as unity plus a positive constant times the square of Chebyshev polynomial  $T_n(x)$ , and that  $n$  characteristic impedance values are sufficient to define the Chebyshev transformer, with the ripple level given by the value of the positive constant.

The fundamental difference between the present study and the transformer studies of Collin's and others is that the device studied here is a spatial filter rather than a frequency filter. If the air spaces  $S_j$  were set equal to zero, this analysis—like Collin's—would also lead to power loss ratios that are even powers of  $\cos k_z t$ . The difference is that in the case of a frequency filter the  $k_0 = 2\pi/\lambda_0$  varies directly with the frequency; in the case of a spatial filter, with  $\epsilon_j$  large compared with unity,  $k_z j$  varies very little over a wide range. Logically, therefore, procedures for designing a spatial filter are not directly analogous to those established for designing quarter-wave transformers.

To consider the spatial domain—assume dielectric constants of the filter media large enough for the  $\theta$ -dependence of the  $k_z j$  in the various layers to be neglected; also assume that the air-dielectric junction characteristics are constant with  $\theta$ . If the thickness of each dielectric layer is a quarter-wavelength at the design frequency and the air-space distance  $S$  between layers is fixed, then the power loss ratios will be even powers of  $\cos(k_0 S \cos \theta)$  or even powers of  $\sin(k_0 S \cos \theta)$ . In such case, the dielectric slab is considered a lumped reactive component; filter synthesis consists in choosing the magnitude of this reactance.

#### 3.2 The Mathematics of Filter Synthesis

The first five Chebyshev polynomials are:

$$T_0(x) = 1,$$

$$T_1(x) = x,$$

$$\begin{aligned}
 T_2(x) &= 2x^2 - 1, \\
 T_3(x) &= 4x^3 - 3x, \\
 T_4(x) &= 8x^4 - 8x^2 + 1.
 \end{aligned} \tag{29}$$

The optimal properties of these polynomials are well known, as are their root locations and in-band and out-of-band characteristics. The functions oscillate with amplitude unity throughout the range and all have the value unit at  $|x|=1$ . The polynomial  $T_m(x)$  has all of its  $m$  zeros within this passband range.

An alternative way of expressing the general polynomial  $T_m(x)$  is:

$$T_m(x) = \cosh(m \cosh^{-1} x). \tag{30}$$

This expression is valid for all  $x$ , but is particularly useful for calculating the stopband polynomial values. Synthesis of spatial filters based on Chebyshev polynomials follows conventional procedure, which begins with the recognition that the power loss ratio is a polynomial in even powers of the sine or cosine of  $(k_0 S \cos \theta)$ . The further specification that the polynomial be one that has  $m$  double zeros within the passband is also common to the theory of filter synthesis, and has the result that the power loss polynomial can be set equal to the expression,

$$A_{11} A_{11}^* = 1 + \Delta^2 T_m^2 \left( \frac{\sin \zeta}{\sin \zeta_1} \right) \tag{31}$$

where

$$\zeta = \frac{2\pi S}{\lambda} \cos \theta.$$

and  $\zeta_1$  is the value of  $\zeta$  at the passband edge.

This expression is unity plus a polynomial of order  $2m$ , with double zeros within the region  $\sin \zeta < \sin \zeta_1$ , and with the maximum ripple  $\Delta^2$  within that band. The expression  $A_{11} A_{11}^*$  has the minimum value unity at the polynomial zeros.

### 3.2.1 TWO-LAYER FILTERS

The coefficient  $A_{11}$  of the wave matrix for a filter made of two identical dielectric slabs of dielectric constant  $\epsilon$  and thickness  $t$  set to a quarter wavelength (in  $\epsilon$ ), computed from Eq. (28), is

$$A_{11} = \frac{1}{S_{21}^2} (e^{j\zeta} - S_{11}^2 e^{-j\zeta}). \tag{32}$$

and  $S_{11}$  and  $S_{21}$  are computed from Eq. (26). Since  $S_{11}$  is real, the power loss ratio is:

$$A_{11} A_{11}^* = 1 + \frac{1}{|S_{21}|^4} (4 S_{11}^2 \sin^2 \zeta). \quad (33)$$

To synthesize a two-layer filter, this ratio is set equal to the expression

$$A_{11} A_{11}^* = 1 + \Delta^2 T_1^2 \left( \frac{\sin \zeta}{\sin \zeta_1} \right). \quad (34)$$

Defining a constant

$$G = \frac{\Delta}{\sin \zeta_1} \quad (35)$$

then leads to the following equation for the dielectric-layer reflection coefficient

$$S_{11} = \frac{-1 + \sqrt{1 + G^2}}{2}. \quad (36)$$

Solving for  $\zeta$  by means of Eq. (36) and selecting the quarter-wave filter thickness for the given  $\epsilon$ , completes the synthesis procedure for given  $\Delta^2$  and  $\sin \zeta_1$ .

### 3.2.2 THREE-LAYER FILTERS

Consider three layers, each a quarter-wave thick at broadside and arranged symmetrically so that the dielectric constant of the central layer is  $\epsilon_2$  and that of the two outer layers is  $\epsilon_1$ , with all layers again separated by the spacing  $S$ . The  $A_{11}$  coefficient of the resulting wave matrix, viewed at the filter input, is

$$A_{11} = \frac{1}{S_{21}(1) S_{21}(2)} \left[ e^{j\zeta} (e^{j\zeta} - S_{11}(1) S_{11}(2) e^{-j\zeta}) + \right. \\ \left. - S_{11}(1) e^{-j\zeta} (S_{11}(2) e^{j\zeta} - S_{11}(1) e^{-j\zeta}) \right]. \quad (37)$$

where the parenthetical (1) and (2) distinguish the parameters for the dielectric layer  $\epsilon_1$  from those of layer  $\epsilon_2$ .

After some manipulation, the power loss ratio can be put into the form:

$$A_{11} A_{11}^* = 1 + \frac{1}{|S_{21}(1)|^4 |S_{21}(2)|^2} \left[ S_{11}(2) + S_{11}(1)^2 S_{11}(2) + \right. \\ \left. - 2 S_{11}(1) + 4 S_{11}(1) \sin^2 \zeta \right]^2. \quad (38)$$

Equating this to

$$1 + \Delta^2 \left( -1 + \frac{2 \sin^2 \zeta}{\sin^2 \zeta_1} \right)^2 \quad (39)$$

yields the following equation for  $S_{11}(1)$ :

$$2S_{11}(1) \sin^2 \zeta_1 - \Delta \left[ 1 - S_{11}^2 \right] \sqrt{1 - \frac{\left[ 4 \cos^4 \zeta_1 S_{11}^2(1) \right]}{\left[ 1 + S_{11}^2(1) \right]^2}} = 0.$$

and then

$$S_{11}(2) = \frac{2S_{11}(1) \cos^2 \zeta_1}{\left[ 1 + S_{11}^2(1) \right]}. \quad (40)$$

### 3.2.3 FOUR-LAYER FILTERS

The coefficient  $A_{11}$  of the wave matrix for a four-layer filter in which the dielectric constant of the two central layers is  $\epsilon_2$  and that of the two outer layers is  $\epsilon_1$  is:

$$A_{11} = \frac{1}{S_{21}^2(1) S_{21}^2(2)} \left[ e^{j\zeta} \left( e^{2j\zeta} - S_{11}(1) S_{11}(2) - S_{11}^2(2) + S_{11}(1) S_{11}(2) e^{-2j\zeta} \right) + - S_{11}(1) e^{-j\zeta} \left( S_{11}(2) e^{2j\zeta} - S_{11}(1) S_{11}^2(2) - S_{11}(2) + S_{11}(1) e^{-2j\zeta} \right) \right]. \quad (41)$$

After substantial manipulation this becomes the following expression for the power loss ratio:

$$A_{11} A_{11}^* = 1 + \frac{\sin^2 \zeta}{\left| S_{21}(1) \right|^4 \left| S_{21}(2) \right|^4} \left\{ 8S_{11}(1) \sin^3 \zeta + \sin \zeta \left[ 2S_{11}^2(1) S_{11}(2) + 2S_{11}(1) S_{11}^2(2) + 2S_{11}(2) - 6S_{11}(1) \right] \right\}^2, \quad (42)$$

which, upon equating to

$$1 + \Delta^2 \left[ 4 \left( \frac{\sin \zeta}{\sin \zeta_1} \right)^3 - 3 \left( \frac{\sin \zeta}{\sin \zeta_1} \right) \right]^2. \quad (43)$$

yields the following equations for defining  $S_{11}(1)$  and  $S_{11}(2)$

$$\frac{2S_{11}(1)}{[S_{21}(1)^2][S_{21}(2)^2]} - \frac{\Delta}{\sin^3 \zeta_1} = 0$$

$$S_{11}(2) = \frac{-[2S_{11}^2(1) + 2] + \sqrt{[2S_{11}^2(1) + 2]^2 + 48S_{11}^2(1)\cos^2 \zeta}}{4S_{11}(1)}. \quad (44)$$

### 3.3 Filter Design

The equations in Sec. 3.2 were derived in terms of  $\sin \zeta$ . Since  $\zeta = (2\pi/\lambda)S \cos \theta$ ,  $\sin \zeta$  is zero at  $(S/\lambda) = n(0.5)$ , with  $n = 0$  excluded as trivial. In principle, therefore, there are a number of different spacings that will allow proper spatial filter synthesis. In practice, the only reasonable spacings for most applications are  $S/\lambda = 0.5$ —sometimes  $S/\lambda = 1.0$ —because larger spacings have a multitude of spatial pass- and stopbands that do not generally suit the given requirements.

For  $S = 0.5\lambda$ , there is a passband ( $\sin \zeta = 0$ ) centered at  $\cos \theta = 1$  (broadside), and also at  $\cos \theta = 0$  (endfire). For  $S = \lambda$  there are passbands at broadside, at  $60^\circ$ , and at endfire. The  $60^\circ$  passband begins just beyond  $40^\circ$ . Thus, the basic filter can be made so as to have synthesized filtering properties from broadside to somewhat beyond  $40^\circ$ , a spacing that is appropriate if the antenna radiation needs no further reduction for large  $\theta$  angles.

Filter synthesis procedure begins with determining the value of  $\zeta_1$  at the end of the passband and the value of some spatial angle variable  $\zeta$  at which a given rejection level is required. Equations (30) and (31) give the out-of-band rejection for Chebyshev filters of the general type. Figures 4 through 6 show the rejection ratios (in decibels) for two-, three-, and four-layer filters for various values of  $\Delta^2$  consistent with rejection ratios of up to 30dB for values of  $\sin \zeta / \sin \zeta_1 < 10$ . From these curves it is possible to choose the value of the passband ripple amplitude  $\Delta^2$  that will provide a given rejection ratio for a specific value of  $\sin \zeta / \sin \zeta_1$ . Since the minimum passband transmission coefficient is  $1/(1 + \Delta^2)$ , the constant  $\Delta^2$  must be kept moderately small if excessive ripple is to be avoided in the passband.

Figures 4 through 6 must be used in conjunction with Figures 7 through 9. In these latter figures, the required reflection coefficients  $S_{11}(1)$  and  $S_{11}(2)$  [computed for two-, three-, and four-layer filters in Eqs.(36), (40), and (44), respectively] are plotted versus the values of  $\sin \zeta_1$  at the end of the passband; the various  $\Delta^2$  values that were used were chosen to cover a range that would give reasonable ripple values while maintaining good filter rejection.

Some interpretation of these figures is necessary to prevent misconceptions. Equation (31) and Figures 4 through 6 are for filters that are synthesized exactly

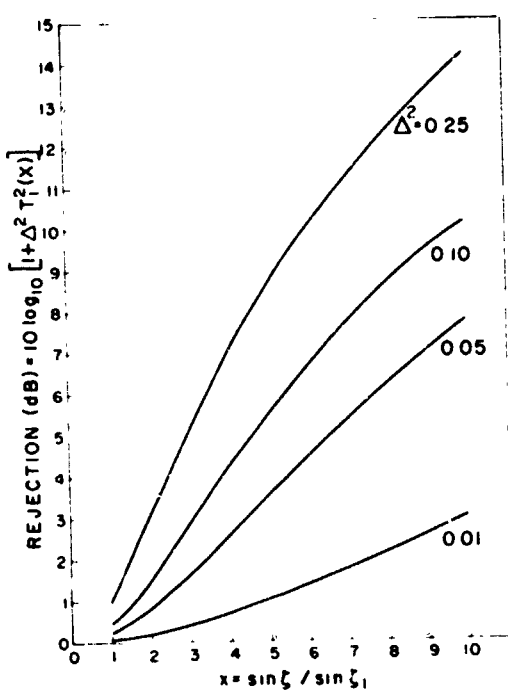


Figure 4. Two-Layer  
Chebyshev Filter Rejection

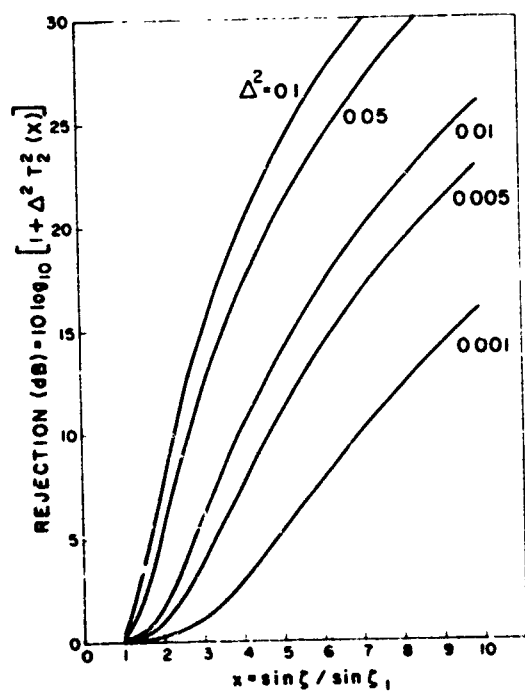


Figure 5. Three-Layer  
Chebyshev Filter Rejection

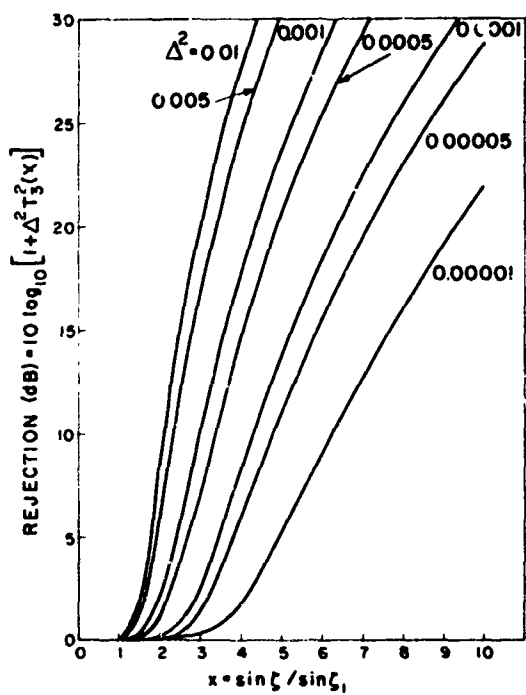


Figure 6. Four-Layer Chebyshev Filter Rejection

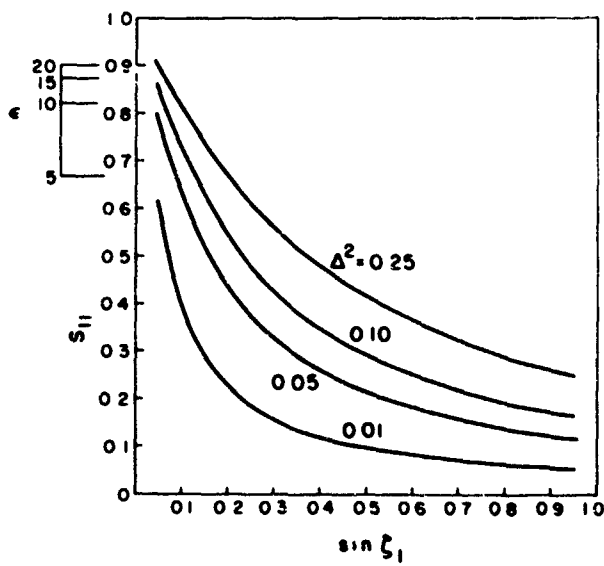


Figure 7. Reflection Coefficients for Two-Layer Chebyshev Filter

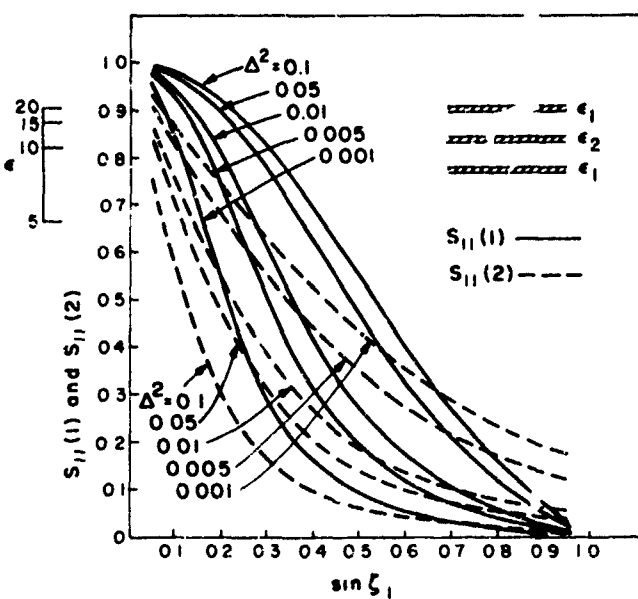


Figure 8. Reflection Coefficients for Three-Layer Chebyshev Filter

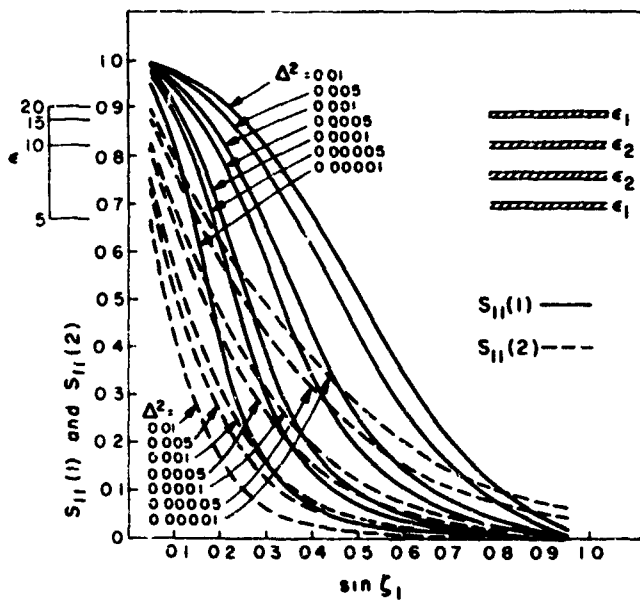


Figure 9. Reflection Coefficients for Four-Layer Chebyshev Filter

like Chebyshev filters, a result not possible in the spatial domain because the reflection and transmission properties of each dielectric slab do vary with  $\theta$ . Under this restriction the filters are not strictly Chebyshev-like in their behavior yet are very nearly so for large  $\epsilon$ . These equations and curves thus represent the idealized Chebyshev filter that has constant slab properties, with values at all angles of  $\theta$  the same as at broadside. They aid in synthesis, but the properties of the actual dielectric filter must be evaluated by considering the exact wave propagation in the structure [using Eq. (18) and the filter scattering parameters obtained from the filter wave matrix, Eq. (27), for each polarization]. Such an analysis is carried out in Sec. 3.4. Similarly, the values of the reflection coefficients plotted in Figures 7 through 9 are for an idealized filter slab with all parameters constant. The horizontal lines indicate these reflection coefficients converted to the values of  $\epsilon$  for quarter-wave slabs at broadside.

The values of the reflection coefficients and those of the dielectric constants of the filter layers are functions of  $\Delta^2$  and  $\text{sin } \xi_1$ , and are not direct functions of  $S/\lambda$ . These figures are thus useful for all  $S$ , since they can easily show how the required dielectric constants depend on the choice of spacing.

### 3.4 Results Obtained With Two Filters

The synthesis procedure described in Sec. 3.3 has been used to derive a number of two-, three-, and four-element filters. The contour plots in Figures 10 and 11 summarize the transmission characteristics of several four-element filters for transmitted and crossed polarizations in generalized  $u, v$  space. These show four-layer filters synthesized subject to the parameters  $\Delta^2 = 0.0004$  and  $\text{sin } \xi_1 = 0.15$ , for  $S = 0.5\lambda$  and  $S = \lambda$ . Since  $\xi$  is unchanged, this choice of parameters leads to filters having identical layers ( $\epsilon_1 = 3.08$ ;  $\epsilon_2 = 15.14$ ), but yielding a different scan performance for each  $S$  value.

The filter transmission factors whose contour plots are represented here are given by  $20 \log_{10}(K)$  for the transmitted polarization, and  $20 \log_{10}(K_{\text{cross}})$  for the cross polarization, where the parameters ( $K$ ) and ( $K_{\text{cross}}$ ) are obtained directly from Eq. (18). The circular contours around the origin in  $u, v$  space indicate that within the passband at least, the filter properties do not depend strongly on the angle  $\phi$ . For larger  $\theta$  values,  $\phi$ -dependence becomes more pronounced and filter behavior is noticeably different, with somewhat more rejection in the H plane ( $v = 0$ ) than in the E plane ( $u = 0$ ). The filter behavior for large scan angles ( $\Theta > 60^\circ$ ) is not plotted for the  $S = 0.5\lambda$  case because of the complexity of the contour plots and the generally unsatisfactory filter performance at such angles.

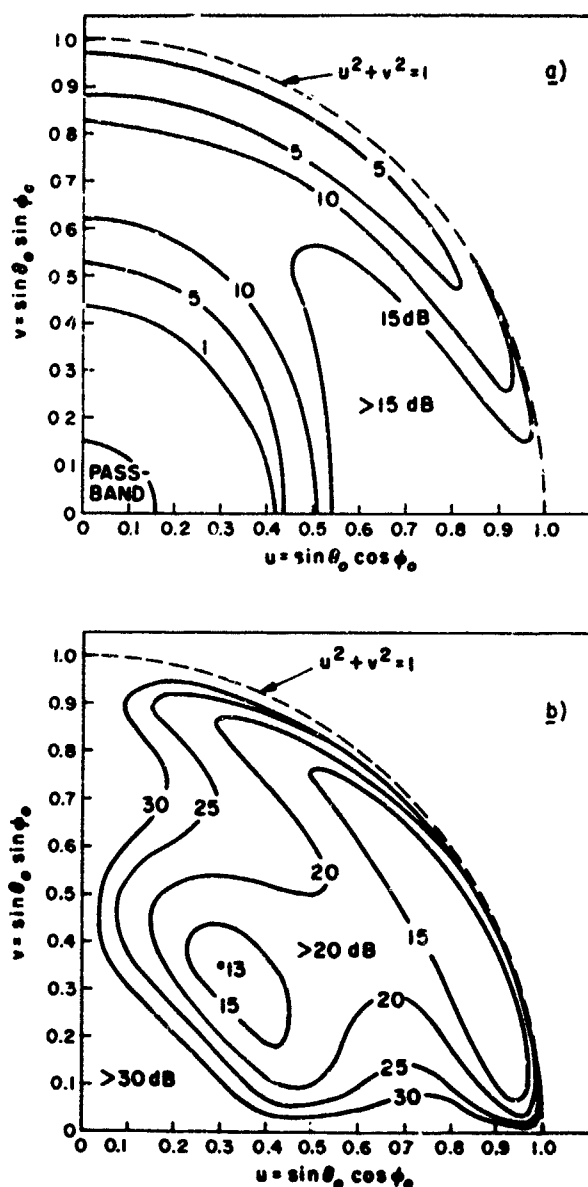


Figure 10. Transmission Characteristics of Four-Layer Chebyshev Filter [ $\epsilon_1 = 3.08$ ;  $\epsilon_2 = 15.14$ ;  $\Delta^2 = 0.0004$ ;  $\sin \zeta_1 = 0.15$ ;  $S = 0.5 \lambda$ ]: (a) Filter Rejection for Transmitted Polarization  $\Phi_0$ ; (b) Isolation Between Transmitted Polarization  $\Phi_0$  and Crossed Polarization  $\Theta_0$

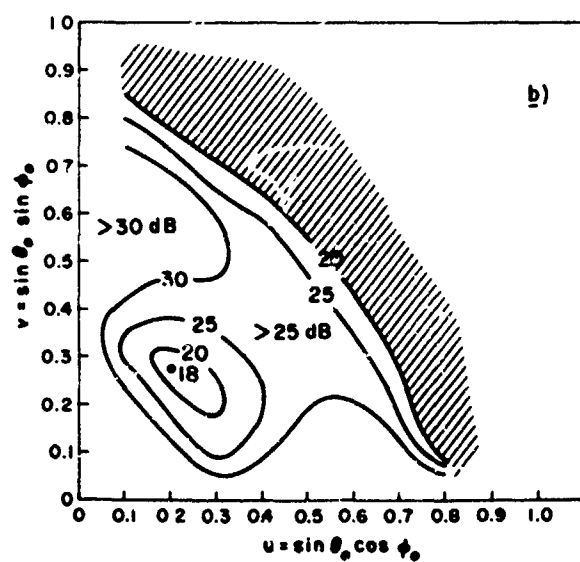
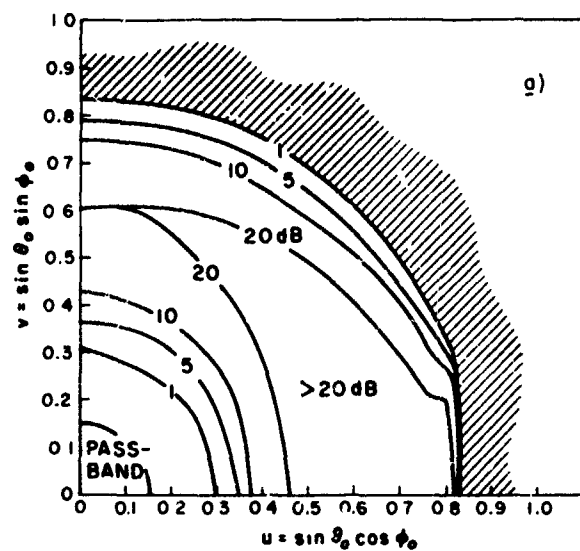


Figure 11. Transmission Characteristics of Four-Layer Chebyshev Filter [ $\epsilon_1 = 3.08$ ;  $\epsilon_2 = 15.14$ ;  $\Delta^2 = 0.0004$ ;  $\sin \zeta_1 = 0.15$ ;  $S = \lambda$ ]: (a) Filter Rejection for Transmitted Polarization  $\Phi_0$ ; (b) Isolation Between Transmitted Polarization  $\Phi_0$  and Crossed Polarization  $\Theta_0$

The comparison of the two cases does illustrate that for given dielectric layers, much sharper filter skirts are possible with  $\lambda$  spacing than with  $0.5\lambda$  spacing. This can be an enormous advantage—if the filter properties beyond about  $\Theta = 50^\circ$  are not important—because the availability, machining properties, and uniformity of materials of lower dielectric constant (less than 15) are far greater than those of materials of higher dielectric constant.

The cross-polarized signal components in Figures 10(b) and 11(b) indicate that these signals are zero in both principal planes, and maximum near  $\phi = 45^\circ$ ; and they are in all cases reduced at least 13 dB by the  $S = 0.5\lambda$  filter, and 18 dB by the  $S = \lambda$  filter. For the specific application considered here, this amount of filtering is more than adequate, but for some other application the cross-polarized transmission may be excessive.

Several filter designs that have spacings between  $0.5\lambda$  and  $\lambda$  have been investigated. Designing  $\sin \zeta$  so that it varies between  $-\sin \zeta_1$  at broadside to  $+\sin \zeta_1$  at the end of the desired radiation sector yields higher  $\sin \zeta / \sin \zeta_1$  ratios and thus greater rejection for given stopband angles. Unfortunately, this choice of  $\zeta_1$  leads to a requirement for excessively high dielectric constants; but when the  $\Delta^2$  value is reduced to one that results in more reasonable dielectric constants the overall filter rejection is increased only slightly over that obtained with the original  $0.5\lambda$  spacing. In such cases there is apparently little to gain by resorting to spacings that are not  $0.5\lambda$  or  $\lambda$ .

### 3.5 Results Obtained With an Array of Parallel-Plane Waveguides

The numerical results of Figures 10 and 11, computed by means of the basic formulas derived in this report, imply incident fields consisting of one or several uncoupled plane waves. The phased array is a more complex distribution. For an infinitely large array, the field is rigorously described in terms of a spectrum of plane waves, some propagating and some cut off (Appendix A). If a stratified filter is used over the array aperture, then the waves reflected by the filter are cross-coupled by the array face. This intercoupled nature of the fields implies that the freespace properties of the filter may be modified by its proximity to the array. Figure 12, however, shows that the dielectric-layer filter can be used for suppressing sidelobes and grating lobes, and so long as the main beam radiation is kept within the filter passband there is relatively little disruption of the basic array properties. It also shows how the two filters of Figures 10 and 11 reduce the residual grating lobes of a special array that incorporates an aperture control technique<sup>7</sup> to eliminate the dominant grating lobe. Arrays of this

7. Mailloux, R. J., and Forbes, G. R. (1973) An array technique with grating-lobe suppression for limited-scan application, IEEE Tr. AP AP-21(No. 5): 597-602, Sept. 1973.

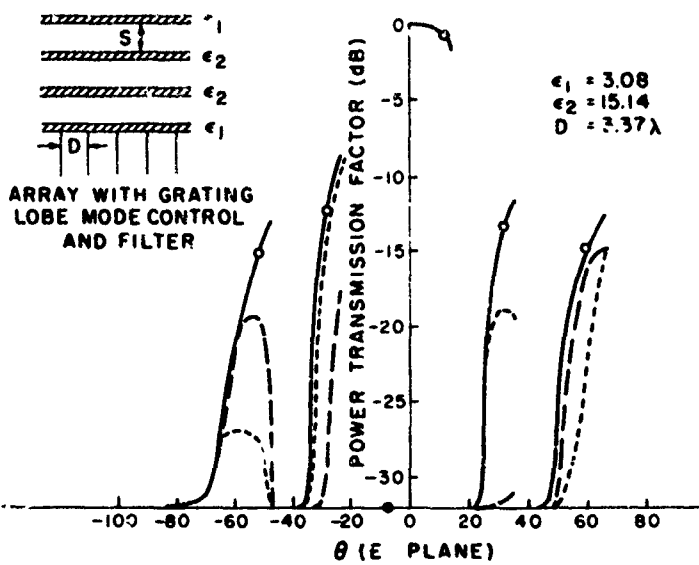


Figure 12. Limited-Scan Array Grating Lobe Amplitude Locus  
 [— odd-mode scanning no filter; - - - odd-mode scanning with four-layer Chebyshev filter ( $S = 0.5\lambda$ ); - - - odd-mode scanning with four-layer Chebyshev filter ( $S = \lambda$ )]

type cannot eliminate all of the grating lobes. The lobes that remain grow with array scan angle, and sometimes get to the -12 dB level at maximum scan. The grating-lobe amplitude loci of an array of parallel-plane waveguides whose inter-element spacings and aperture width are both  $3.17\lambda$  are given by the solid curves of Figure 12. The maximum scan point  $11.5^\circ$  is denoted by a circle at each of the grating lobe loci. The broken and dashed curves are for the filters of Figures 10 and 11, respectively.

A comparison of these curves shows that even in the presence of mutual coupling of the elements in the array, the rejection ratios for the filters placed directly on the actual array are almost identical with those of the isolated filter. The rejection properties of the  $S=\lambda$  filter are particularly appropriate to the given array: all of the near grating lobes are reduced by substantial factors. The remaining grating lobe, near  $60^\circ$  at maximum scan, appears approximately at the second filter passband and so is relatively unaltered by the filter. In practice, this lobe is further reduced by the projection factor of the finite array, and would appear at about the -18 dB level with or without the filter. Thus, the filter of Figure 11 reduces all grating lobes to approximately -18 dB, and reduces all but the  $60^\circ$  grating lobe to about -20 dB. This is accomplished with a four-layer Chebyshev design using materials of moderate dielectric constant.

#### 4. CONCLUSIONS

The practicality of a new technique for Chebyshev synthesis of spatial filters has been demonstrated. The filters designed to test the theory have given good control of sidelobes, especially in phased-array antennas, where they can be used as radomes as well. They are particularly valuable in the limited-scan arrays of precision-approach radar (PAR) systems.

#### References

1. Collin, R. E. (1955) Theory and design of wideband multisection quarter-wave transformers, Proc. IRE 43(No. 2):179-185, Feb. 1955.
2. Cohn, S. B. (1955) Optimum design of stepped transmission-line transformers, IRE Tr. MTT MTT-3(No. 2):16-21, Apr. 1955.
3. Riblett, H. J. (1957) General synthesis of quarter-wave impedance transformers, IRE Tr. MTT MTT-5(No. 1):36-43, Jan. 1957.
4. Young, L. (1959) Tables for cascaded homogeneous quarter-wave transformers, IRE Tr. MTT MTT-7(No. 2):233-244, Apr. 1959.
5. Young, L. (1962) Stepped-impedance transformers and filter prototypes, IRE Tr. MTT MTT-10(No. 5):339-359, Sept. 1962.
6. Collin, R. E. (1960) Field Theory of Guided Waves, McGraw-Hill, pp. 79-93.
7. Mailloux, R. J., and Forbes, G. R. (1973) An array technique with grating-lobe suppression for limited-scan application, IEEE Tr. AP AP-21(No. 5): 597-602, Sept. 1973.

## Appendix A

### Radiated Field of Infinite Array

The radiated field of an infinite array of the linearly polarized rectangular apertures shown in Figure 1 is given in Eq.(A1) in terms of a single-component hertzian potential. The main beam of the array is steered to the angles  $\theta_0, \phi_0$ .

$$\begin{aligned}\bar{\mathbf{E}}(\bar{\mathbf{r}}) &= -j\omega \nabla \times [\bar{\Pi}(x, y, z)], \\ \bar{\mathbf{B}}(\bar{\mathbf{r}}) &= \nabla [\nabla \times \bar{\Pi}(x, y, z)] + k^2 \bar{\Pi}(x, y, z); \end{aligned} \quad (\text{A1})$$

where

$$\bar{\Pi}(x, y, z) = \hat{x} \Pi_x(x, y, z).$$

The potential function  $\Pi_x$  is given by:

$$\Pi_x(x, y, z) = \frac{1}{\omega D_x D_y} \sum_{m=-\infty}^{\infty} \sum_{n=-\infty}^{\infty} \frac{e^{-jk_{mn} \cdot \bar{r}}}{K_{mn}} \int_S [\hat{z} \times \bar{\mathbf{E}}(x', y')] e^{jk_{mn} \cdot \bar{r}'} dx' dy', \quad (\text{A2})$$

where  $D_x$  and  $D_y$  are the interelement spacings in the  $x$  and  $y$  directions,

$$\bar{k}_{mn} = k_0 \left( \hat{x} u_m + \hat{y} v_n + \hat{z} \frac{K_{mn}}{k_0} \right),$$

and

$$\bar{r} = \hat{x}x + \hat{y}y + \hat{z}z;$$

and where  $\bar{E}(x', y')$  is the aperture field, linearly polarized in the  $y$  direction;  $\vec{r}$  is a position vector in  $x, y, z$  coordinates, and  $\vec{r}'$  is measured in the aperture ( $z' = 0$ ).

The direction cosines  $u$  and  $v$  for the specified grating lobe positions  $u_m, v_n$  for a main beam at  $u_o = \sin \theta_o \cos \phi_o$  and  $v_o = \cos \theta_o \sin \phi_o$  are defined by:

$$\begin{aligned} u_m &= u_o + m/D_x, \\ v_n &= v_o + n/D_y. \end{aligned} \quad (A3)$$

The values  $m$  and  $n$  define propagating waves for all integers for which the parameter

$$K_{mn} = k_o \sqrt{1 - u_m^2 - v_n^2} \quad (A4)$$

is real. Thus, a set of waves is defined, some propagating and some cut off. The propagating waves travel in the direction of the allowed  $\bar{k}_{mn}$  values and are plane; for these,  $K_{mn}$  reduces to  $k_o \cos \theta_o$ . The potential function  $\Pi_x$  can thus be written as the spectrum:

$$\Pi_x(x, y, z) = \sum_{m,n} \Pi_{mn}(x, y, z), \quad (A5)$$

and the field components of this plane wave spectrum for the wave at  $u_m, v_n$  are:

$$\begin{aligned} B_{xmn} &= k_o^2 (1 - u_m^2) \Pi_{mn}, & E_{xmn} &= 0, \\ B_{ymn} &= -k_o^2 u_m v_n \Pi_{mn}, & E_{ymn} &= -\omega K_{mn} \Pi_{mn}, \\ B_{zmn} &= -k_o^2 u_m \frac{K_{mn}}{k_o} \Pi_{mn}. & E_{zmn} &= \omega k_o v_n \Pi_{mn}. \end{aligned} \quad (A6)$$

In conventional phased arrays the spacings  $D_x$  and  $D_y$  are specified to exclude all but the wave associated with the main beam ( $\theta_o, \phi_o$ ), but certain special-purpose arrays intended for limited sector-scanning allow a small number of grating lobes to propagate. The spatial filters described in this report reduce and control such lobes.

The magnitude of the electric field for the  $m, n$  mode is given by

$$k_o \omega \sqrt{1 - u_m^2} \Pi_{mn}.$$

and since this parameter multiplies each wave it will now be defined as  $C(\theta_{mn}, \phi_{mn})$ .

## Appendix B

### Wave Matrix Definitions for Parallel and Perpendicular Polarization

Figure 2 schematically shows the signal parameters that are related by the wave matrix. Conventionally, the incident electric field is chosen as the reference signal, with the wave matrix expressing the linear relation between input and output parameters as:

$$\begin{pmatrix} a_1 \\ b_1 \end{pmatrix} = \begin{pmatrix} A_{11} & A_{12} \\ A_{21} & A_{22} \end{pmatrix} \begin{pmatrix} a_2 \\ b_2 \end{pmatrix}. \quad (B1)$$

The coefficients in  $A$  are related to the conventional scattering matrix coefficients by the following definitions:

$$\begin{aligned} A_{11} &= \frac{1}{T_1}, & A_{21} &= \frac{\Gamma_1}{T_1}, \\ A_{12} &= -\frac{\Gamma_1}{T_1}, & A_{22} &= T_2 - \frac{\Gamma_1 \Gamma_2}{T_1}; \end{aligned} \quad (B2)$$

for the scattering parameters defined:

$$\begin{aligned}\Gamma_1 &= \frac{b_1}{a_1} \Bigg|_{b_2=0}, & \Gamma_2 &= \frac{a_2}{b_2} \Bigg|_{a_1=0}, \\ T_1 &= \frac{a_2}{a_1} \Bigg|_{b_2=0}, & T_2 &= \frac{b_1}{b_2} \Bigg|_{a_1=0}.\end{aligned}\quad (B3)$$

When the transmission lines for ports 1 and 2 have the same characteristic impedance, then  $T_1 = \Gamma_2$  (reciprocity). Otherwise, this relationship does not hold unless, as Collin shows,<sup>6</sup> the signal amplitudes are normalized so that the power in a wave of amplitude  $a_i$  is given by  $a_i a_i^*$ . Throughout the following analysis, these amplitudes are defined to be the E field parallel to the dielectric junction, and thus  $T_1 \neq T_2$  except when the two ports are located in layers of the same  $\epsilon$ .

Incident fields for both polarizations are given in Eq. (13). Since the projection of  $\hat{\theta}$  onto the plane of the junction involves the factor  $k_{z_0}/k_0$  in the incident medium (air) and is  $k_{z_i}/k_i$  in a material of dielectric constant  $\epsilon_i$ , where

$$k_i = k_0 \sqrt{\epsilon_i}$$

and

$$k_{z_i} = k_0 \sqrt{\epsilon_i - \sin^2 \theta_{\text{inc}}}, \quad (B4)$$

then this projection factor is used to multiply the field vector that lies in the plane of incidence in order to find the tangential component at the interface. For parallel polarization the incident  $B_\phi$  is  $(k_0/\omega) E_\theta$  and the incident tangential  $\bar{E}$  is  $(k_{z_0}/k_0) E_\theta$ . For perpendicular polarization the  $E_\phi$  is the tangential  $\bar{E}$  field and the tangential  $\bar{B}$  field is  $(-k_0/\omega) E_\phi$ .

Similar projections apply within any dielectric layer. For parallel polarization the equations for continuity of tangential  $\bar{E}$  and  $\bar{B}$  fields at the interface between two media of dielectric constants  $\epsilon_1$  and  $\epsilon_2$ , for incident and reflected wave amplitudes ( $\bar{E}_1 = E_\theta$ ) and  $E_2$  in medium 1, and  $E_3$  and  $E_4$  in medium 2, are:

$$\begin{aligned}(k_{z_1}/k_1)(E_1 + E_2) &= (k_{z_2}/k_2)(E_3 + E_4), \\ k_{\epsilon_1}(E_1 - E_2) &= k_{\epsilon_2}(E_3 - E_4).\end{aligned}\quad (B5)$$

Then, defining signal amplitudes  $a_1$ ,  $b_1$ ,  $a_2$ ,  $b_2$  as  $(k_{z_i} k_i)$  times the E-field amplitudes  $E_1$  through  $E_4$  yields the following equations relating the tangential E fields at the boundary:

$$(a_1 + b_1) = (a_2 + b_2)$$

and

$$(a_1 - b_1) = (z_1 z_2)(a_2 - b_2). \quad (B6)$$

where

$$z_j = (k_{z_i}/k_j^2 \cos \theta_{inc}).$$

(The  $\cos \theta_{inc}$  is included to remove the angle dependence of  $z_j$  for the trivial  $\epsilon_2 = \epsilon_1$  case where  $k_{z_j} = k_0 \cos \theta_{inc}$ .)

Following a similar procedure for perpendicular polarization yields the tangential  $\bar{E}$  and  $\bar{B}$  equations

$$E_1 + E_2 = E_3 + E_4.$$

$$k_{z_1}(E_1 - E_2) = k_{z_2}(E_3 - E_4). \quad (B7)$$

Then, defining  $a_1$ ,  $b_1$ ,  $a_2$ , and  $b_2$  to be equal to  $E_1$  through  $E_4$  yields the same equation as for parallel polarization, but with

$$z_j = \frac{\cos \theta_{inc}}{k_{z_j}}. \quad (B8)$$

For either case, Eq. (B1), when transformed into wave matrix form, becomes

$$\begin{pmatrix} a_1 \\ b_1 \end{pmatrix} = \frac{1}{T_1} \begin{bmatrix} 1 & \Gamma_1 \\ \Gamma_1 & 1 \end{bmatrix} \begin{pmatrix} a_2 \\ b_2 \end{pmatrix}, \quad (B9)$$

where

$$\Gamma_1 = \frac{(1 - z_1/z_2)}{(1 - z_1/z_2)}$$

and

$$T_1 = 1 + \Gamma_1.$$

where  $\Gamma_1$  and  $T_1$  are the junction reflection and transmission coefficients. The junction reflection coefficient  $\Gamma_2$ , seen from medium 2, is the negative of  $\Gamma_1$ ; and  $T_2 = 1 + \Gamma_2 = 1 - \Gamma_1$ .